NOx Storage in Barium-Containing Catalysts

Erik Fridell,*,[1] Magnus Skoglundh,* Björn Westerberg,*,† Stefan Johansson,*,‡ and Gudmund Smedler*

*Competence Centre for Catalysis, Chalmers University of Technology, SE 412 96 Göteborg, Sweden; †Department of Chemical Reaction Engineering, Chalmers University of Technology, SE 412 96 Göteborg, Sweden; and ‡Department of Applied Physics, Chalmers University of Technology, and Göteborg University, SE 412 96 Göteborg, Sweden

The effect of key parameters on the characteristics of barium oxide-based NO_x storage catalysts was systematically investigated. Model $Pt/BaO/Al_2O_3$, BaO/Al_2O_3, $Pt–Rh/Al_2O_3$, and $Pt–Rh/BaO/Al_2O_3$ catalysts were prepared and evaluated with respect to NO_x storage capacity using transient flow reactor studies, temperature-programmed desorption studies (TPD), and *in situ* Fourier transform infrared (FTIR) absorption spectroscopy. The influence of temperature, storage and regeneration times, NO_x source (NO or NO_2), oxygen concentration, reducing agent (C_3H_6, C_3H_8, CO, or H_2), and carbon dioxide concentration on NO_x storage capacity was studied. Significant amounts of NO_x were found to be stored in the catalysts containing both barium oxide and noble metals. For these catalysts the following observations were made: (1) maximum NO_x storage was observed at about 380°C; (2) around this temperature no significant differences between NO and NO_2 on NO_x storage capacity could be observed; (3) a slow increase in stored NO_x could be observed with increasing oxygen concentration during the lean phase; (4) significant NO_x desorption peaks, mainly of NO, were observed immediately after the switch from lean to rich conditions; and (5) at about 380°C the *in situ* FTIR spectra show characteristic nitrate peaks in the region 1300–1400 cm^{-1} when NO_x was stored under lean conditions and isocyanate peaks around 2230 cm^{-1} when the catalysts were regenerated under rich conditions in the presence of hydrocarbons. The step leading to stored NO_x is believed to involve NO_2 and the presence of atomic oxygen. During the rich period, the noble metal surfaces are probably reduced, leading to breakthrough peaks when NO desorbs. © 1999 Academic Press

1. INTRODUCTION

Increasing awareness of the need to reduce emissions of carbon dioxide into the atmosphere has led to great pressure on automobile manufacturers to reduce the fuel consumption of their products. One way to improve the fuel economy of gasoline-fueled cars is to use engines that operate at lean conditions, rather than at the normal stoichiometric air/fuel ratios. Depending on driving conditions a lean-burn engine can decrease fuel consumption by up to 30% compared with a stoichiometric engine (1).

When the exhaust contains a mixture of oxygen and the pollutants hydrocarbons, carbon monoxide, and nitrogen oxides, close to stoichiometric conditions, as is the case for most gasoline-fueled cars today, the pollutants can be almost completely transformed to carbon dioxide, water, and dinitrogen in a three-way catalyst. However, the exhaust from a lean-burn engine contains a large surplus of oxygen which prevents the reduction of nitrogen oxides. This requires the development of new catalytic techniques for reduction of lean-burn engine NO_x emissions. Different catalytic systems have been developed for continuous reduction of NO_x under lean conditions using specific combinations of reducing agents and catalyst compositions (2–4). A different concept to solve this problem is the NO_x storage catalyst (5–7). This catalyst is used in an engine that operates alternatively under lean or rich conditions. During lean operation, the nitrogen oxides in the exhaust are stored in the catalyst. As the NO_x storage capacity of the catalyst becomes saturated it is necessary to regenerate the catalyst by turning the engine to rich conditions for a short period whereupon the stored NO_x is released and subsequently reduced over noble metal sites.

NO_x reduction for mixed lean conditions was reported by Takahashi *et al.* (6) using a NO_x storage catalyst with noble metals (mainly Pt), alkaline earth metals (mainly Ba), and alumina. They found that the amount of NO_x stored increased with increasing oxygen content in the gas. They also reported evidence of stored NO_x in the form of nitrates from IR studies. It was also concluded that the reduction of NO_x to N_2 during rich conditions takes place on noble metal sites. Bögner *et al.* (7) investigated the NO_x conversion properties of a NO_x storage catalyst using both synthetic gas mixtures and engine exhaust. They concluded that their catalyst stores NO_x as a surface metal nitrate and that the catalyst becomes fully regenerated under rich conditions.

A model NO_x storage catalyst washcoat comprises three essential parts: (i) a high-surface-area substrate material, (ii) noble metals that catalyze oxidation and reduction reactions, and (iii) a NO_x storage component. The substrate is normally γ-alumina with a surface area of typically

[1] To whom correspondence should be addressed. Fax: +46 31 7722967. E-mail: fridell@fy.chalmers.se.

200 m^2/g. The noble metal loading usually includes both platinum for oxidation reactions and rhodium to increase reduction reaction rates. Several metal oxides (mainly alkaline earth metal oxides) have proven effective in forming nitrates with NO$_2$, which decompose at high temperatures (8). This usually produces NO and O$_2$. If these nitrates can be made to decompose at 300–600°C, the metal oxides may be used for reversible storage of NO$_x$. Examples of such metals are barium and strontium.

The reaction sequence in the NO$_x$ storage/release cycle has been discussed in other publications (7, 9). It is generally assumed that oxidation of NO to NO$_2$ is a necessary initial step before NO$_x$ storage can take place during lean conditions. Assuming BaO to be the storing component, the storage would then take place by, e.g.,

$$2NO_2 + O + BaO \rightarrow Ba(NO_3)_2. \qquad [1]$$
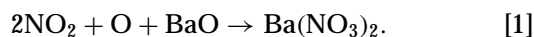
However, this simple step already includes several uncertainties and, further, may be the sum of several elementary reaction steps. It may be possible to achieve storage directly with NO rather than NO$_2$, although NO$_2$ is the more likely candidate. Inclusion of atomic oxygen on the left side of reaction [1] is needed for mass balance reasons but has not been proven experimentally. This would mean a further involvement of Pt as a provider of atomic oxygen. The nature of the barium complex is in reaction [1] assumed to be BaO, though other barium compounds such as hydroxides and carbonates may be present depending on temperature and gas composition. Finally, the nature of the stored NO$_x$–barium complex is not well known. Takahashi *et al.* (6) report it to be in the form described in reaction [1].

The decomposition of the stored NO$_x$ during the rich period can be assumed to be the reverse of reaction [1] so that NO$_2$ and NO are released and subsequently reduced over noble metal (essentially Rh) sites by the reducing agent. Following this assumption, the kinetics of the storage and decomposition will essentially be determined by the rates of reaction [1] and the reverse reaction for the varying conditions (gas composition and temperature).

This study focuses on gaining the basic understanding still lacking with respect to NO$_x$ storage mechanisms. We have therefore used model samples containing alumina as substrate, platinum and rhodium as noble metals, and barium oxide as the storage compound. We used a simplified synthetic exhaust gas normally containing oxygen, propene, and nitrogen oxides together with an inert carrier gas. Flow reactor studies were performed under various conditions, normally with transients between lean and rich conditions. Further, results from temperature-programmed desorption (TPD) of nitrogen oxides as well as *in situ* Fourier transform infrared (FTIR) absorption spectroscopy studies are presented.

2. METHODS

Flow reactor studies were performed using monolith samples with an alumina washcoat, a storage compound (BaO), and noble metals (Pt, Rh). To elucidate the importance of the various ingredients, samples were also prepared without storage compound or noble metals, respectively. For the FTIR studies, corresponding powder catalysts were pressed into thin disks.

Monolith samples of cordierite, $2MgO \cdot 2Al_2O_3 \cdot 5SiO_2$, with a length of 15 mm and a cross section consisting of 69 channels, with 64 channels/cm^2, were impregnated with an ammonia solution (pH 11.8) (10), and immersed in an alumina slurry, prepared by dispersing 32.0 g γ-Al$_2$O$_3$ and 8.0 g boehmite in 130 g distilled water and 30 g diluted nitric acid (1 mol/dm^3). The monolith sample was then blown dry with hot air (95°C) for 5 min and sequentially calcined in air at 550°C for 10 min to fixate the alumina onto the monolith walls. The procedure was repeated until the desired amount of alumina (160 mg for the Ba-containing samples and 200 mg for the catalysts without barium oxide) was deposited on each sample. The applied alumina washcoat was finally stabilized by calcination in air at 550°C for 90 min (10).

Some of the samples were then impregnated by dipcoating with barium nitrate [Ba(NO$_3$)$_2$ pro analysi, from Aldrich] solution (10). The impregnated support was dried at 95°C and then calcined at 600°C for 90 min. The impregnation procedure was repeated until the content of the formed oxide was 40 mg. The noble metals, Pt and Rh, were applied by direct impregnation, i.e., by filling the monolith channels with chloride solutions of platinum or rhodium (H$_2$PtCl$_6$ and RhCl$_3$, respectively, both of pro analysi grade from Johnson Matthey), and drying in air at 95°C for 2 h, and finally calcining in air at 550°C for 45 min. This process oxidizes the barium presumably to barium oxide. The fresh catalysts were reduced in H$_2$ at 450°C for 35 min and stabilized in the lean gas mixture at 550°C for 2 h. The compositions of the three monolith samples used in this work are given in Table 1.

The powder sample for the FTIR studies was prepared by dissolving Ba(NO$_3$)$_2$ in distilled water. γ-Al$_2$O$_3$ 8.0 g was added under continuous stirring and the pH was adjusted to 10.0 by addition of NH$_4$OH. The sample was then freeze-dried and calcined in air at 600°C for 60 min. A platinum solution was prepared by dissolving [Pt(NH$_3$)$_4$]Cl$_2 \cdot$ H$_2$O in distilled water, resulting in a concentration of 27.5 mg Pt/g solution. A 2.9-g amount of the sample was added to 100 g distilled water under continuous stirring. Pt solution 2.19 g was added and the pH was adjusted to 10.0 by addition of NH$_4$OH. The sample was then kept under stirring for 60 min. Finally the sample was freeze-dried and calcined at 550°C for 2 h. The composition of the sample is given in Table 1.

TABLE 1

Composition, BET Surface Area, and Estimated Noble Metal Dispersion for the Samples

	Rh (wt%)	Pt (wt%)	BaO (wt%)	Al_2O_3 (wt%)	Dispersion	BET surface area (m^2/g)
Pt–Rh/BaO/Al_2O_3 monolith	1.0	2.0	20	77	0.18	30.3
Pt–Rh/Al_2O_3 monolith	1.0	2.0	0	97	0.27	31.9
BaO/Al_2O_3 monolith	0	0	20	80	NA	30.0
Pt/BaO/Al_2O_3 powder	0	2.0	20	78	—	—

Specific areas of the catalysts determined by nitrogen adsorption according to the BET method (Digisorb 2600 instrument, Micromeritics) are given in Table 1.

The flow reactor used in most experiments is described elsewhere (10). Briefly, it consists of a horizontal quartz tube encased in a divisible tubular furnace. The catalyst is sealed in the middle of the heated zone with quartz wool and the gases are introduced via mass flow controllers. Temperatures are measured at two places: in the reactant gas flow 11 mm before the catalyst, and inside one of the monolith channels 1 mm from the catalyst front. Reactant and product gases are analyzed on-line with respect to total hydrocarbon content (VE5 flame ionization detector, JUM Engineering), CO_2 content (UNOR 6N IR detector, Maihak), NO and NO_2 content (CLD 502 chemiluminescence detector, Tecan), and N_2O content (UNOR 610 IR detector, Maihak). The gas mixtures used are indicated in Table 2. The space velocity was kept constant at about 54,000 h^{-1}.

The TPD measurements were performed with the same monolith samples in a different quartz flow reactor described elsewhere (11, 12). A mass spectrometer continuously probes a fraction of the reactant and product gases. The temperature is measured in the middle of one of the central channels in the monolith sample. The mass spectrometer is always calibrated by measuring known gas mixtures. The samples were either prereduced (4% H_2 in Ar) or preoxidized (5% O_2 in Ar) at 500°C for 5 min. They were then exposed to 1% NO or NO_2 in Ar at a flow of 100 ml/min for 5 min at room temperature prior to a heating ramp (40°C/min) in Ar flow. The noble metal dispersion of the samples was estimated from NO TPD measurements on prereduced samples assuming one adsorption site per noble metal atom in the surface layer (see Table 1).

The FTIR experiments were performed with thin disks (approximately 15 mg/cm^2) of catalyst in a reaction chamber with CaF_2 windows. The disk was fixed in a folded tungsten grid placed in the middle of the reaction chamber. The temperature was measured with a thermocouple, in contact with the grid, and controlled via the voltage applied over the grid.

The fresh catalysts were reduced in 30% H_2 in N_2 (total flow rate of 100 ml/min) at 450°C for 30 min, stabilized in a gas mixture with 5% O_2, 1000 ppm NO, and 3000 ppm C_3H_6 in N_2 (total flow rate 1000 ml/min) for 30 min, and finally degassed in N_2 (1000 ml/min) at 550°C for 30 min.

The FTIR experiments were performed at a total flow rate of 1000 ml/min. In the storage experiments a lean gas mixture (5% O_2, 400 ppm NO, and 900 ppm C_3H_6 in N_2) and a rich gas mixture (400 ppm NO and 900 ppm C_3H_6 in N_2) were used. The same respective gas concentrations were used in the experiments in which switching between different reactant combinations occurred.

TABLE 2

Gas Concentrations for the Reactor Experiments^a

	NO(NO_2) (ppm)	C_3H_6 (ppm)	O_2 (%)
Flow reactor			
Lean	300–1100	900	8
Rich	300–1100	900	0
FTIR			
Lean	400	900	5
Rich	400	900	0

^{a} The different gas compositions were balanced with nitrogen to maintain constant flow (1450 ml/min for the monolith experiments and 1000 ml/min, for the FTIR experiments) during the rich and lean gas phases.

3. RESULTS

3.1. Temperature Ramps

The NO, NO_2, N_2O, NO_x (NO + NO_2), N_{bal} (NO_x + $2N_2O$), and CO_2 signals during a reactant-temperature ramp with a constant lean gas mixture (i.e., without transients) over the Pt–Rh/BaO/Al_2O_3 catalyst are shown in Fig. 1a. Hydrocarbon light-off can be observed around 250°C, where the CO_2 signal rapidly increases. A maximum
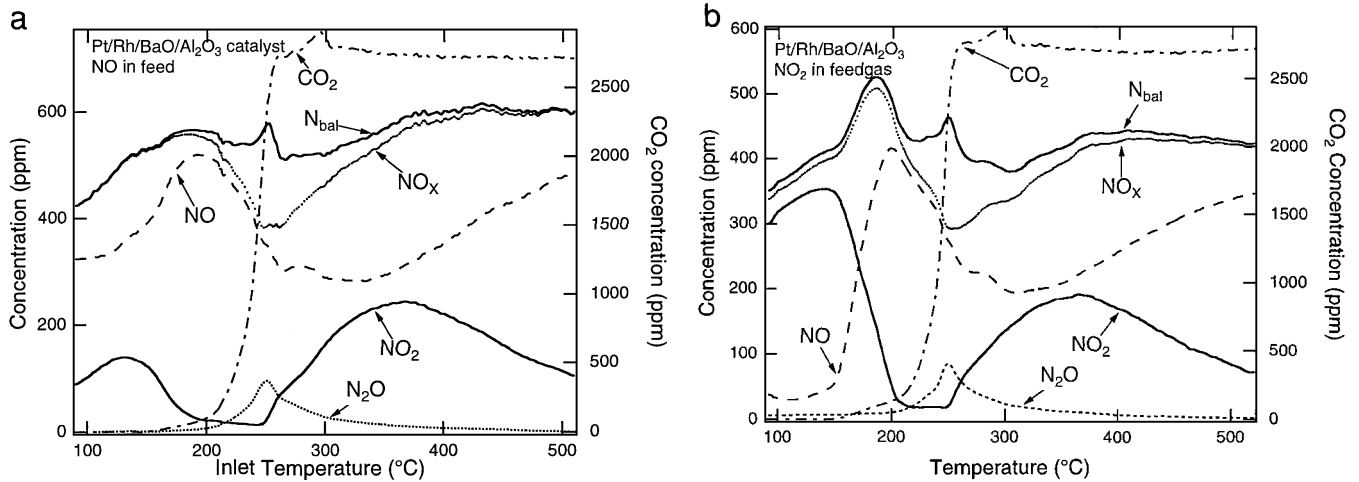
FIG. 1. (a) Concentrations of NO, NO$_2$, N$_2$O, NO$_x$ (NO + NO$_2$), N_{bal} (NO$_x$ + 2N$_2$O), and CO$_2$ for a heating ramp (5°C/min) in a gas mixture of 600 ppm NO, 900 ppm C$_3$H$_6$, and 8% O$_2$ over the Pt–Rh/BaO/Al$_2$O$_3$ catalyst. (b) Same as in (a) but with NO replaced by 400 ppm NO$_2$.

in NO oxidation to NO$_2$ occurs around 375°C. Reduction of NO$_x$ to N$_2$O and N$_2$ takes place in the temperature interval 200–350°C with a maximum in NO$_x$ reduction of about 30% at 250°C. The N$_2$O formation maximizes at the same temperature at which about 42% of the reduced NO$_x$ leaves the catalyst as N$_2$O. The formation of N$_2$ can be observed from the N_{bal} curve in Fig. 1. It is very small in the whole temperature interval. Figure 1b shows a corresponding experiment but with NO$_2$ in the feed instead of NO. Around 150°C, the NO$_2$ is reduced by propene to form NO under these conditions (observe the slight increase in CO$_2$ concentration). There is also a NO$_x$ desorption peak around these temperatures. Above 200°C, the results in Figs. 1a and 1b are very similar; i.e., in this part of these experiments it is not important if the introduced NO$_x$ is the form of NO or NO$_2$. Similar experiments with Pt–Rh/Al$_2$O$_3$ catalyst with the same noble metal load give a significantly more pronounced light-off behavior with a CO$_2$ overshoot, higher N$_2$O production, and significant NO desorption at light-off. For the BaO/Al$_2$O$_3$ sample, on the other hand, no light-off behavior was observed. A transition from NO$_2$ to NO in the product gas takes place around 400°C and only about 20% of the propene is oxidized, even at 500°C.

3.2. Transients in the Feed Gas Composition

3.2.1. General. For the NO$_x$ storage catalyst to be effective, it must be used in connection with transients in the gas composition; i.e., during lean-burn periods NO$_x$ is stored in the catalyst and during short periods of rich conditions, the stored NO$_x$ is released and subsequently reduced. Figure 2a shows the NO and NO$_2$ concentration traces in the product gas over a Pt–Rh/BaO/Al$_2$O$_3$ catalyst during such transients. The inlet temperature was 400°C and the transient conditions are described in Table 2. The difference

between the lean (NO$_x$ storing) phase and the rich (regenerating) phase in this case is that the oxygen content in the gas is turned on and off, respectively (and compensated by changes in the N$_2$ flow to maintain a constant total flow). When O$_2$ is switched on, for example, at 320 s in Fig. 2a, there is a relatively slow increase in both the NO and NO$_2$ signals. The reason for this slow increase is that NO$_x$ is being stored in the catalyst. The amount of NO$_x$ stored is thus the integrated difference between an imagined rapid increase in the NO and NO$_2$ signals (this behavior is seen when using a catalyst without a storage compound; see Fig. 2b) and the measured increase (multiplied by the molar flow). For example, the amount of NO$_x$ stored during the lean phase between $t_1 = 320$ s and $t_2 = 560$ s in Fig. 2a is

$$S_{NO_x} = \left(n_{NO_2}(t_2) + n_{NO}(t_2) \right)(t_2 - t_1)$$
$$- \int_{t_1}^{t_2} \left(n_{NO_2} + n_{NO} \right) dt - 2 \int_{t_1}^{t_2} n_{N_2O}\, dt \quad [2]$$

times the molar flow, where n_i is the measured concentration in the product gas. The last term accounts for the formation of N$_2$O (which is very small in Fig. 2a). In principle, a term accounting for the formation of N$_2$ should be included. We have found this production to be small during the lean phase for most of the experiments presented here (see Fig. 1).

During the rich phase, all NO$_x$ is being effectively reduced by the C$_3$H$_6$. Also, the NO$_x$ stored in the catalyst during the previous lean phase is released and reduced. Breakthrough peaks can be seen mainly for NO when switching from lean to rich conditions. These features are commented on below. The reduction of NO$_x$ in the lean phase is negligible at 400°C and this oxygen concentration (see Fig. 1). The formation of nitrous oxide (N$_2$O) can be observed when switching from lean to rich conditions and vice versa. The
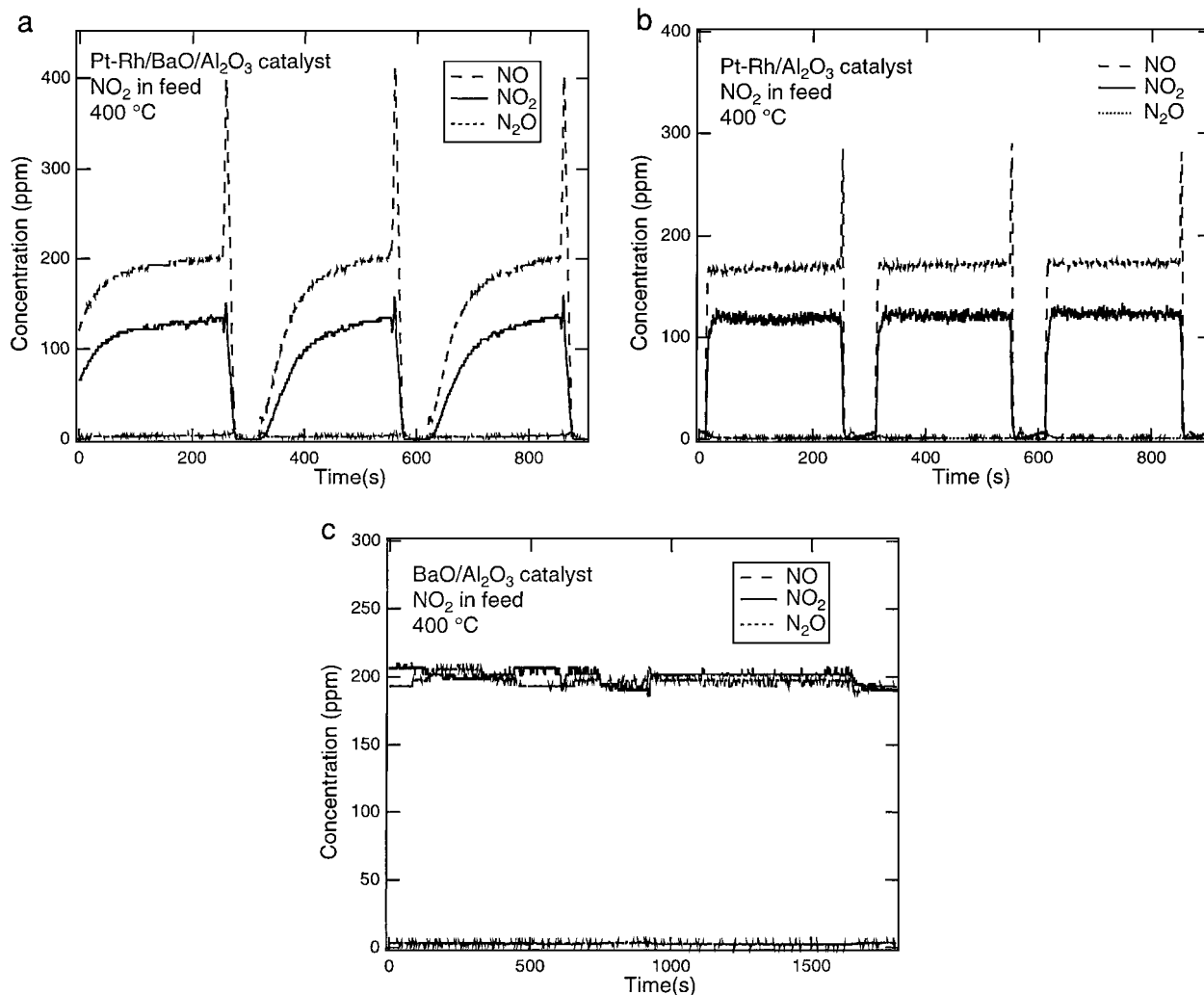
FIG. 2. (a) NO, NO₂, and N₂O signals resulting from the reaction over the Pt–Rh/BaO/Al₂O₃ catalyst at 400°C with gas mixtures described in Table 2 (340 ppm NO₂) for transients with a 240-s lean phase and a 60-s rich phase. (b) Same as in (a) but for the Pt–Rh/Al₂O₃ catalyst and 300 ppm NO₂. (c) Same as in (a) but for the BaO/Al₂O₃ sample and 400 ppm NO₂.

HC signal (not shown) is effectively zero during the lean phase. A HC breakthrough peak is present when switching from rich to lean conditions. There is a temperature decrease within the catalyst of about 15°C during the rich phase compared with the lean phase under these conditions.

When performing similar cycles with a catalyst containing no specific NO_x storage component, i.e., a Pt–Rh/Al₂O₃ catalyst, no storage of NO_x can be observed when analyzing the product gas (Fig. 2b). Breakthrough peaks from desorbing NO, similar to those in Fig. 2a, can be observed for this sample as well. There is also N₂O formation on switching between lean and rich conditions. For a sample without Pt–Rh but with BaO, there is no storage or release and only minor reduction (during the rich phase) takes place (Fig. 2c).

One question concerns the role of the NO oxidation step in the storage of NO_x. The transients presented in Figs. 2a–2c were performed with NO₂ in the feed gas rather than NO.

There is, however, no significant difference in these results compared with similar data for NO in the feed.

3.2.2. Influence of temperature. The NO_x signal during storage transients is measured at different temperatures under the conditions described in Table 2 (with NO in the feed). The amount of NO_x stored during each lean phase is presented versus temperature in Fig. 3 for the range 280–520°C, together with the initial rate (the average storage rate during the first 20 s of a lean phase) of storage when switching from rich to lean conditions. In this temperature interval, a maximum in NO_x storage is seen at around 380°C and a very low value is measured above 500°C. The rate appears to maximize at somewhat higher temperatures. Also shown are the corresponding storage values when using NO₂ in the feed gas rather than NO. The latter appear similar to those with NO.
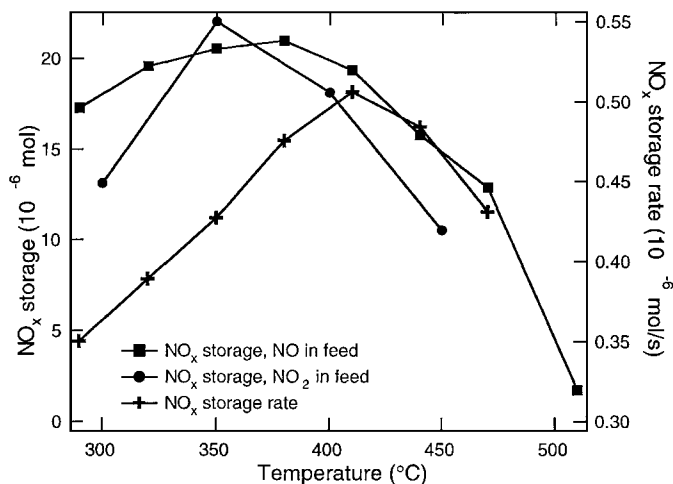
FIG. 3. Amount of NO_x stored during a lean period (as in Fig. 1a) in the Pt–Rh/BaO/Al$_2$O$_3$ catalyst as a function of temperature with either NO or NO$_2$ in the feed together with the initial NO_x storage rate with NO in the feed.

3.2.3. Influence of gas composition on storage capacity. The influence of O$_2$ content during the lean phase on NO_x storage over Pt–Rh/BaO/Al$_2$O$_3$ is illustrated in Fig. 4 and Table 3. The experiment was done by using a lean phase containing 13% O$_2$ for two storage–reduction cycles followed by two cycles with 8% O$_2$ and so on down to 0.26% O$_2$. Only one of the cycles at each oxygen content is shown in Fig. 4. As seen in this figure, the NO$_2$-to-NO ratio during the lean phase increases with increasing oxygen content in the gas while the NO_x level is independent of the oxygen content down to 1.4% O$_2$. At lower oxygen content, NO_x is reduced by C$_3$H$_6$ also during the lean phase. Under reducing conditions the nitrogen oxides are reduced by the hydrocarbons and no NO_x is recorded in the product
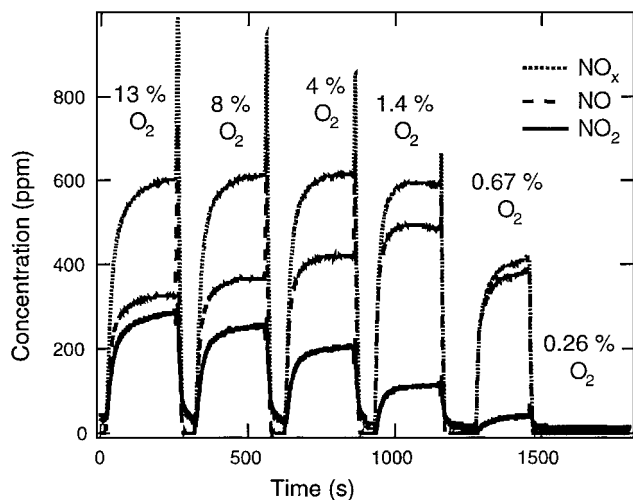

FIG. 4. NO, NO$_2$, and NO_x signals resulting from the reaction over the Pt–Rh/BaO/Al$_2$O$_3$ catalyst with different oxygen contents during the lean phase, 600 ppm NO, 900 ppm C$_3$H$_6$ at $T = 400°$C.

TABLE 3

Amount of NO$_x$ Stored at Different Oxygen Concentrations in the Lean Phase from the Data in Fig. 4

O$_2$ content (%)	Amount of NO$_x$ stored ($\times 10^{-6}$ mol)
13	13.5
8	10.2
4	9.2
1.4	9.8

gas. Under slightly lean conditions (0.67 vol% O$_2$) the NO and NO$_2$ signals do not start to increase immediately after switching to lean conditions. This occurs probably because there is an induction time after turning on the oxygen flow before all the adsorbed hydrocarbons are oxidized, i.e., before the local composition on the catalyst switches from rich to lean. While there are still hydrocarbons on the catalyst surface, the adsorbed NO_x is reduced and the storage does not start until enough oxygen is supplied to give oxidizing conditions.

The influence of C$_3$H$_6$ partial pressure on NO_x storage was also investigated and the results are presented in Table 4. As can be seen, storage varied only slightly with propene content. Storage is observed even if the C$_3$H$_6$ is turned off but the process of regeneration and reduction is then much slower. [This type of transient is thoroughly discussed in a forthcoming publication (13)]. There are NO_x breakthrough peaks of similar magnitude observed at all C$_3$H$_6$ levels examined.

The influence on NO_x storage with addition of carbon dioxide to the gas stream at 400°C is presented in Table 5. Apparently the amount of NO_x stored is somewhat decreased by the presence of CO$_2$ at this temperature.

The effect of using different reducing agents during the storage–reduction cycles is illustrated in Table 6 for propene (900 ppm), propane (810 ppm), carbon monoxide (8100 ppm), and hydrogen (8100 ppm). The experiment was done using the same S value [oxidizing–reducing character as defined by Summers and Baron (14)] of 19.8 during the lean phase and therefore different fractions of the respective reducing agent in the gas stream were used. As

TABLE 4

Amount of NO$_x$ Stored in One Lean Period for Different Propene Concentrations

C$_3$H$_6$ content (ppm)	Amount of NO$_x$ stored ($\times 10^{-6}$ mol)
133	11.6
267	12.3
667	11.0
1333	10.3

TABLE 5

Amount of NO_x Stored with Addition of CO_2

CO_2 content (%)	Amount of NO_x stored ($\times 10^{-6}$ mol)
0	21.6
4.2	18.0
8.3	16.3
12	16.1

can be seen there is little difference in the amounts of NO_x stored with respect to the reducing agent used. One must in this context realize that the rich periods are relatively long (60 s) compared with what would be realistic for a lean-burn engine. A greater influence of the choice of reducing agent may be expected with shorter regeneration times.

The influence on NO_x storage yield of addition of small amounts of oxygen (up to 0.5%) during the rich phase during a standard lean–rich cycle was found to be negligible. Also, when different reducing agents were used, no difference in the amounts of NO_x stored in the following lean phase was observed as discussed above. However, a somewhat less effective initial reduction during the rich phase was seen with CO, compared with the other reducing agents.

Regeneration of the catalyst is more effective if no nitrogen oxides are present during the rich phase. Further, the catalyst can be regenerated by thermal desorption of NO_x. Both of these phenomena are shown in Fig. 5, which illustrates a sequence in which the catalyst is regenerated in different ways. The amounts of NO_x stored in the respective following lean phases are listed in Table 7. Considerably more NO_x is stored after regeneration in a rich NO_x-free atmosphere than for the standard regeneration procedure (with NO_x and C_3H_6 present) used in this work. The amount of NO_x, that can be seen to desorb in the atmosphere containing only inert gas is about 12 μmol which can be compared with the stored amount of 30 μmol NO_x.

3.2.4. Influence of phase duration. The influence of the storage and regeneration times on NO_x storage over a Pt–Rh/BaO/Al$_2$O$_3$ catalyst at 400°C is summarized in Table 8.

TABLE 6

Amount of NO_x Stored during a Lean Period for Different Reducing Agents

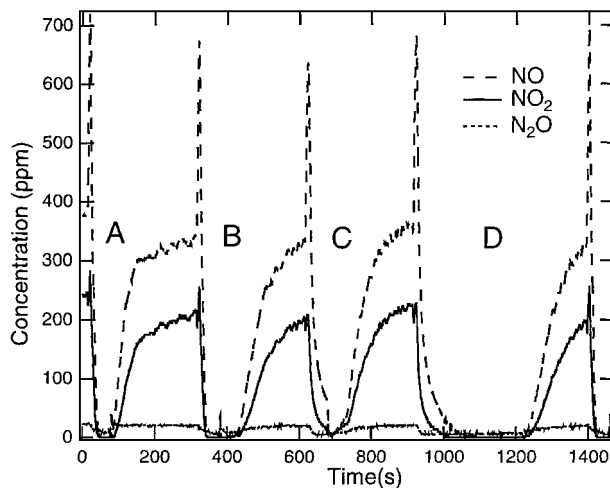| Reducing agent	Amount of NO_x stored ($\times 10^{-6}$ mol)
C_3H_6	21.6
C_3H_8	21.8
CO	20.3
H_2	21.2

FIG. 5. Transients with the Pt–Rh/BaO/Al$_2$O$_3$ catalyst regenerated in different ways: (A) NO and C_3H_6 for 60 s, (B) C_3H_6 for 60 s, (C) inert gas for 60 s, (D) inert gas for 240 s. The lean-phase gas mixture contained NO, C_3H_6, and O_2. Concentrations as in Table 2. $T = 400$°C.

For the regeneration conditions used, the catalyst is completely regenerated after $<$40 s; i.e., longer regeneration times do not influence the amount of NO_x stored during the subsequent lean phase. Storage reaches saturation after about 200 s under these conditions.

3.2.5. Breakthrough peaks. There are breakthrough peaks in the NO_x signal, consisting mainly of NO, when switching from the storage phase to the regeneration phase. Regarding these peaks the following observations can be made: First, they show a significant increase in magnitude with temperature. Second, as can be seen in Fig. 4, they show an increase in magnitude with increasing oxygen content in the lean-phase gas stream. Third, when the propene fraction in the feed gas was varied from 100 to 1300 ppm, the magnitude of the peaks remained constant. Fourth, peaks are also seen for catalysts without BaO, i.e., Pt/Al$_2$O$_3$ and Pt–Rh/Al$_2$O$_3$ catalysts. Fifth, neither the length of the storage phase nor the length of the rich phase influences peak heights.

TABLE 7

Amount of NO_x Stored after the Different Regenerating Procedures in Fig. 5

Conditions for rich period	Amount of NO_x stored ($\times 10^{-6}$ mol) during subsequent lean period
NO + C_3H_6, 60 s (A)	17.4
C_3H_6, 60 s (B)	34.4
Inert, 60 s (C)	29.9
Inert, 240 s (D)	40.6
Amount of NO_x ($\times 10^{-6}$ mol) desorbed during (D)	12.2

TABLE 8

Amount of NO$_x$ Stored for Different Storage and Regeneration Periods

Lean period (s)	rich period (s)	Amount of NO$_x$ stored ($\times 10^{-6}$ mol)
240	60	11.8
240	40	12.0
240	20	10.1
240	10	4.5
240	5	2.1
960	60	11.1
480	60	12.1
240	60	11.8
120	60	10.0
60	60	9.1

3.3. TPD Measurements

Temperature-programmed desorption measurements were performed for the NO$_x$ storage catalyst with Pt–Rh/Ba/Al$_2$O$_3$ and for samples without either the storage component (BaO) or the noble metals, respectively. TPD was done by exposing both prereduced and preoxidized samples to NO or NO$_2$ at room temperature. Figure 6a shows the TPD spectra after dosing NO at room temperature on a prereduced Pt–Rh/BaO/Al$_2$O$_3$ catalyst. As can be seen the NO is reduced on the surface as manifested in the N$_2$ and N$_2$O peaks at around 200°C. The N$_2$O signal decreases rapidly above 200°C while N$_2$ desorbs during the entire temperature interval investigated. The only trace of NO is a small peak around 90°C. The result of a similar experiment but with a preoxidized sample is shown in Fig. 6b. In this case no reduction of NO took place; there is a small NO peak at around 90°C and a larger one at about 500°C. There is also an O$_2$ peak around 500°C. It is possible that an oxygen layer on the noble metals prevents the dissociation of NO. It is also possible that an oxygen layer prevents the adsorption of NO. The sum of the integrated N-containing peaks is much larger for the prereduced catalyst than for the preoxidized one (compare Figs. 6a and 6b). When NO$_2$ rather than NO was dosed at room temperature, a much larger quantity was adsorbed. Furthermore, prereduced and preoxidized samples show similar TPD spectra, indicating that the strong oxidizing agent NO$_2$ oxidizes the sample at room temperature. The resulting spectra are shown in Fig. 6c. Two NO$_2$ peaks are present: one at around 100°C and a larger one around 400°C. There are NO and O$_2$ peaks around 450°C, probably due to decomposition of desorbed NO$_2$ over noble metal sites.

TPD measurements were also performed on the Pt–Rh/Al$_2$O$_3$ sample and the BaO/Al$_2$O$_3$ sample. Figures 6d and 6e show NO TPD spectra of the prereduced and preoxidized Pt–Rh/Al$_2$O$_3$ catalysts, respectively. The prereduced catalyst produces N$_2$ and N$_2$O with peaks at 280 and 250°C, re-

spectively. There is also some NO desorption at lower temperatures. Compared with Fig. 6a, there is somewhat more N$_2$ and especially N$_2$O. For the preoxidized catalyst, no reduction of NO is observed and NO and O$_2$ desorb with major peaks at around 100 and 400°C, as well as an additional NO feature at 300°C. The major desorption peaks of NO and O$_2$ are thus shifted approximately 100°C compared with what is the case for the preoxidized Pt–Rh/BaO/Al$_2$O$_3$ catalyst (Fig. 6b). The NO$_2$ TPD spectrum for the Pt–Rh/Al$_2$O$_3$ catalyst is shown in Fig. 6f. Again, prereduced and preoxidized samples produce the same desorption products. Two major NO$_2$ desorption peaks can be seen: one around 150°C and one around 350°C. Some of the NO$_2$ desorbing at the higher temperature decomposes to form O$_2$ and NO.

The corresponding TPD results for the BaO/Al$_2$O$_3$ sample are shown in Figs. 6g, 6h, and 6i. There is no reduction of NO on this noble metal-free sample for any case. In both NO TPD experiments, NO can be seen to desorb from the catalyst. Some O$_2$ desorption can also be seen from the preoxidized sample. The NO$_2$ TPD spectra show NO$_2$ desorption as well as some O$_2$ desorption around 500°C.

3.4. FTIR Measurements

Figure 7a shows two spectra of Pt/BaO/Al$_2$O$_3$ exposed to a lean and a rich mixture for 5 min at 250°C. Figures 7b–7f show corresponding spectra at 290, 330, 370, 410, and 450°C. The major features are bands associated with nitrates, carbonates, and isocyanate (15). There are also smaller bands associated with nitrite, nitro, and carboxylate groups (15). The assignments are summarized in Table 9. When comparing the spectra measured at different temperatures a general trend is observed. The bands in the region 1200–1700 cm^{-1} are larger at 250°C and diminish when the temperature is increased. It can also be observed, at each

TABLE 9

FTIR Peak Assignments

| Wavenumber (cm^{-1})	Assignment [according to (15)]
1555, 1250	Nitrate, monodentate, degenerate asymmetric stretch
1545, 1295	Nitrate, bidentate, degenerate asymmetric stretch
1215	Nitrite, bridged
1395	Nitro, asymmetric stretch
1310	Nitro, symmetric stretch
1460	Carbonate, monodentate, asymmetric stretch
1320	Carbonate, monodentate, symmetric stretch
1575	Carbonate, bidentate, C=O stretch
1245	Carbonate, bidentate, asymmetric stretch
1620	Carbonate, bridged, C=O stretch
1280	Carbonate, bridged, asymmetric stretch
1635	Carboxylate, asymmetric stretch
1410	Carboxylate, symmetric stretch
2230	Isocyanate, degenerate stretch
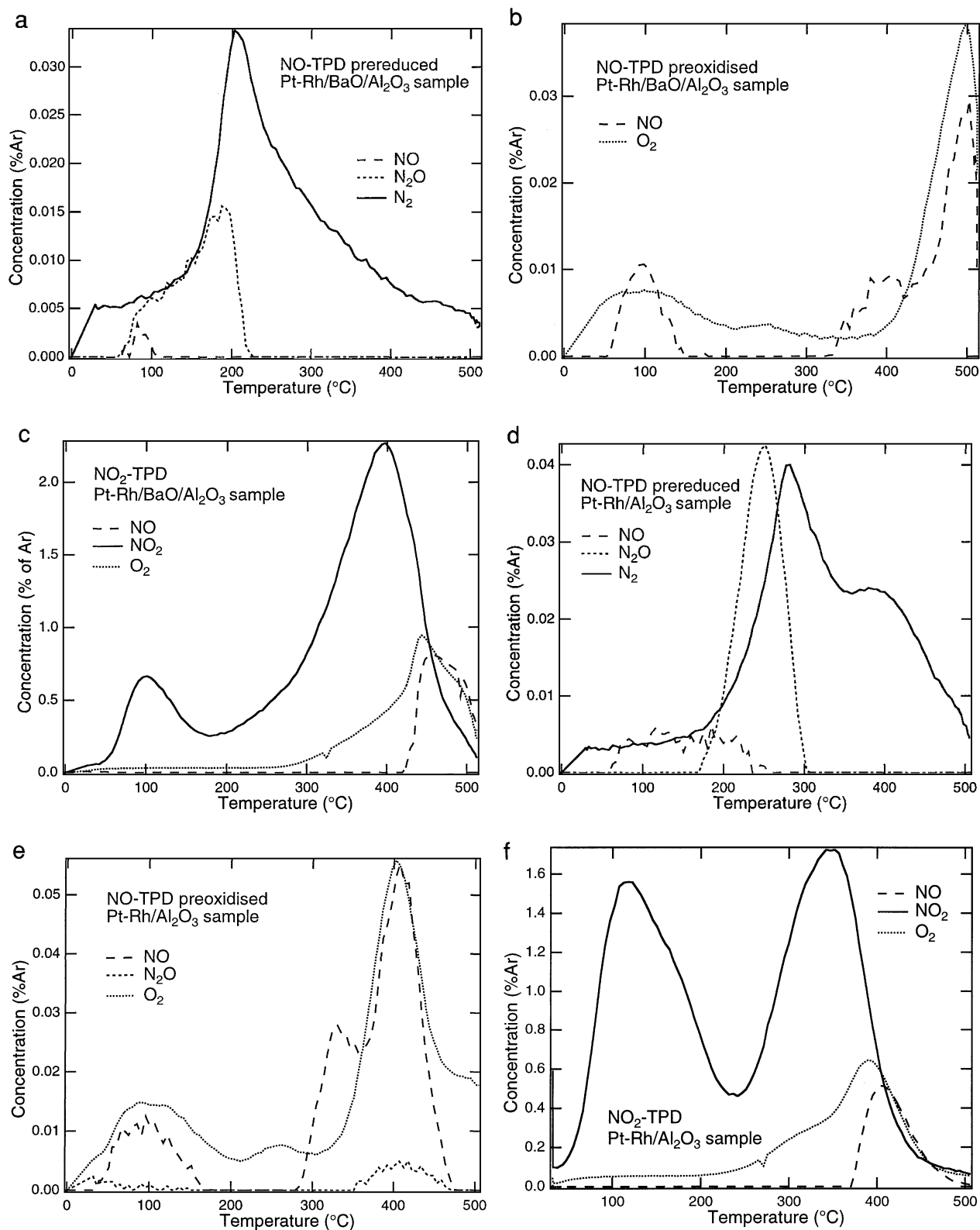
FIG. 6. NO and NO$_2$ TPD measurements: (a) NO on a prereduced Pt–Rh/BaO/Al$_2$O$_3$ sample. (b) NO on a preoxidized Pt–Rh/BaO/Al$_2$O$_3$ sample. (c) NO$_2$ on a Pt–Rh/BaO/Al$_2$O$_3$ sample. (d) NO on a prereduced Pt–Rh/Al$_2$O$_3$ sample. (e) NO on a preoxidized Pt–Rh/Al$_2$O$_3$ sample. (f) NO$_2$ on a Pt–Rh/Al$_2$O$_3$ sample. (g) NO on a prereduced BaO/Al$_2$O$_3$ sample. (h) NO on a preoxidized BaO/Al$_2$O$_3$ sample. (i) NO$_2$ on a BaO/Al$_2$O$_3$ sample.

g

NO-TPD prereduced BaO/Al$_2$O$_3$ sample

-- NO

Concentration (%Ar)

Temperature (°C)

h

NO-TPD preoxidised
BaO/Al$_2$O$_3$ sample

-- NO
⋯ O$_2$

Concentration (%Ar)

Temperature (°C)

i

NO$_2$-TPD BaO/Al$_2$O$_3$ sample

-- NO
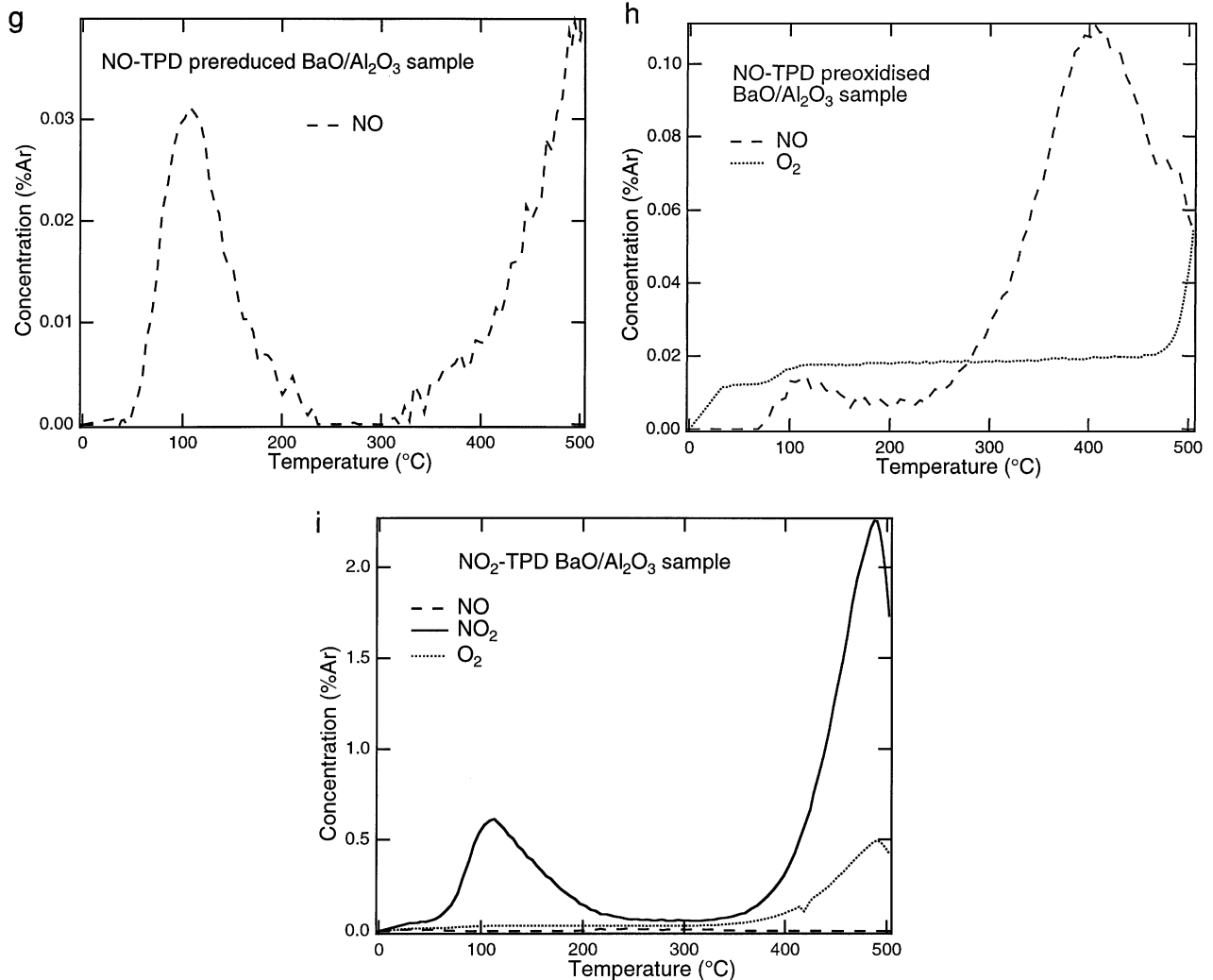— NO$_2$
⋯ O$_2$

Concentration (%Ar)

Temperature (°C)

FIG. 6—*Continued*

temperature, that the bands in the spectra measured in a lean mixture are larger than the bands in the spectra measured in a rich mixture (except for the isocyanate band at 2250 cm^{-1}). The difference in the nitrate bands at 1545 and 1555 cm^{-1} between the spectra measured in a lean mixture and the spectra measured in a rich mixture indicates the amount of NO$_x$ stored during a cycle with 5 min of lean conditions and 5 min of rich conditions. From this it can be seen that the amount of NO$_x$ stored reaches a maximum at 370°C. In an analogous way the amount of CO$_2$ stored can be determined by the carbonate band at 1460 cm^{-1}. It is observed that the amount of CO$_2$ stored is greatest at 250°C. The isocyanate band, which is negligible during the lean phase, is also very temperature dependent, with a maximum around 410°C.

Figure 8 shows the spectra of Pt/BaO/Al$_2$O$_3$ during an experiment with constant NO and C$_3$H$_6$ concentrations and in which the oxygen content have been increased from 0.2%

to 0.4, 0.8, 2, 4, and finally 8%, with 5 min at each oxygen concentration. The spectra for 0.2, 0.4, and 0.8% O$_2$ were similar and therefore only the spectrum for 0.8% O$_2$ is shown. At 0.2, 0.4, and 0.8% oxygen, there are mainly carbonate bands. These bands grow weakly with oxygen content between 0.2 and 0.8%. When the oxygen content is increased to 2%, both nitrate and carbonate bands grow markedly and bands associated with nitro and carboxylate groups become apparent. The nitrate, nitro, carbonate, and carboxylate bands continue to grow when the oxygen content is increased to 4%. These bands also continue to grow when the oxygen content is increased to 8%, but not as much as between 2 and 4% oxygen.

4. DISCUSSION

The experimental results presented above show that NO$_x$ can be stored in a catalyst containing barium and noble
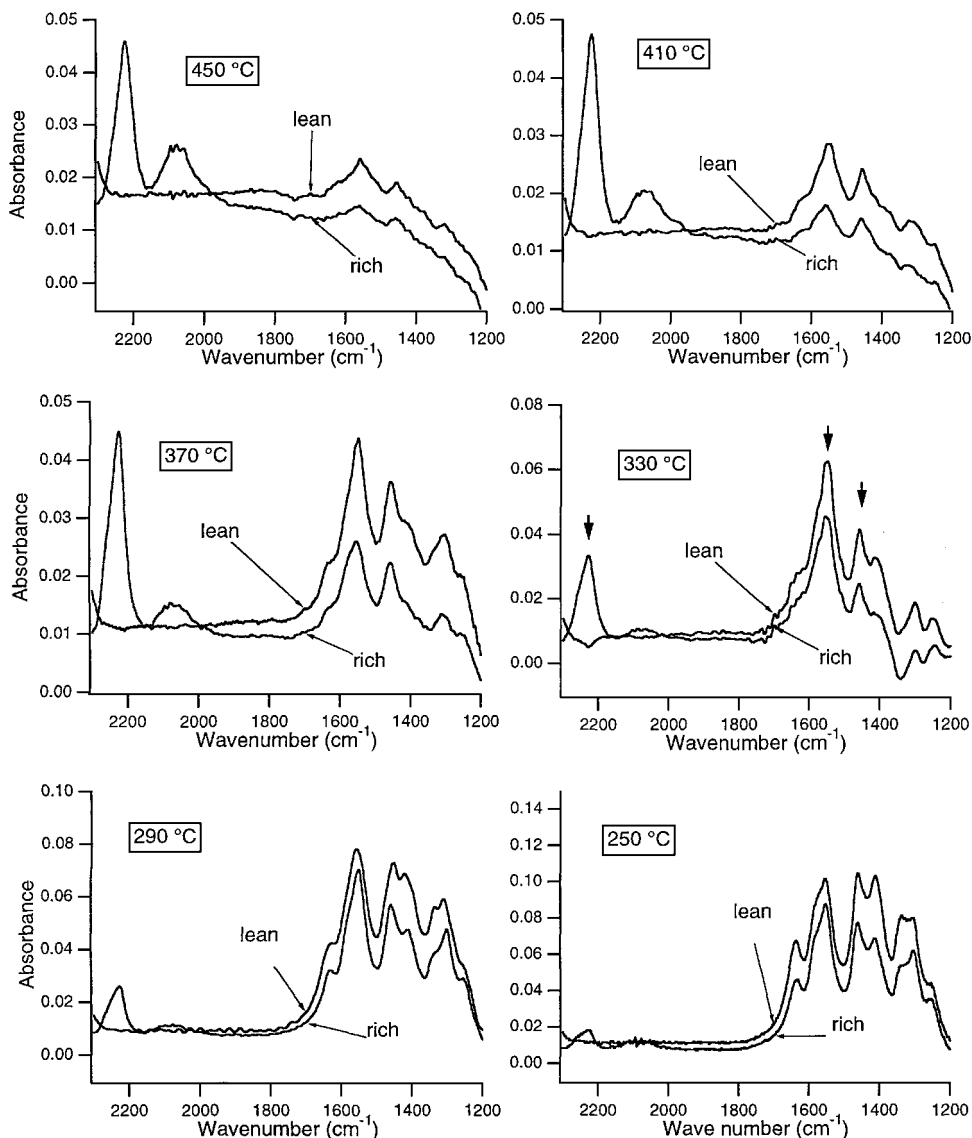
FIG. 7. *In situ* FTIR spectra for lean and rich conditions (see Table 2) for a Pt/BaO/Al$_2$O$_3$ sample at different temperatures. Major bands associated with NCO (2230 cm^{-1}), nitrates (1545, 1555 cm^{-1}), and carbonates (1460 cm^{-1}) are marked by arrowheads for $T = 330°$C.
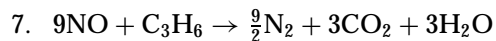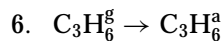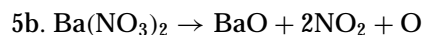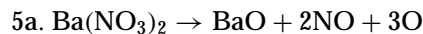
metals under lean conditions. During a subsequent rich phase the stored NO$_x$ is released and reduced.

One NO$_x$ storage–reduction cycle can be assumed to comprise the following steps:

For lean conditions:

1. $NO^g \rightarrow NO^a$
2. $O_2^g \rightarrow 2O^a$
3. $NO^a + O^a \rightarrow NO_2$
4a. $2NO + 3O + BaO \rightarrow Ba(NO_3)_2$
4b. $2NO_2 + O + BaO \rightarrow Ba(NO_3)_2$

For rich conditions:

5a. $Ba(NO_3)_2 \rightarrow BaO + 2NO + 3O$
5b. $Ba(NO_3)_2 \rightarrow BaO + 2NO_2 + O$
6. $C_3H_6^g \rightarrow C_3H_6^a$
7. $9NO + C_3H_6 \rightarrow \frac{9}{2}N_2 + 3CO_2 + 3H_2O$

This is a somewhat simplified reaction scheme. For example, NO$_2$ adsorption and desorption and NO desorption are not included. Further, the NO$_x$ reduction, steps 6 and 7, is of course only an example of many possible pathways. It should also be noted that some of the steps (notably 4a, 4b, 5a, and 5b) are in reality the sum of several substeps. However, we believe that the essential parts of the NO$_x$ storage–reduction cycle can be understood from this scheme.
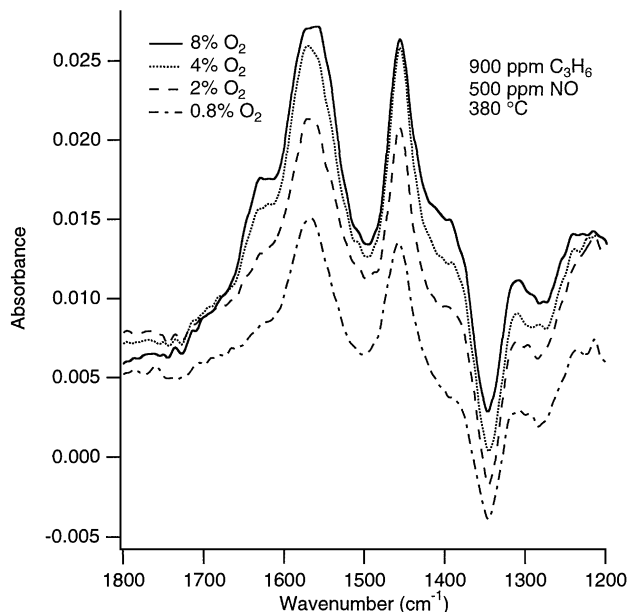
FIG. 8. *In situ* FTIR spectra for a Pt/BaO/Al$_2$O$_3$ catalyst with different oxygen concentrations at 380°C.

The importance of NO$_2$ as a precursor to stored nitrate was assumed by Bögner *et al.* (7) and Takahashi *et al.* (6). From our data we know that the storage of NO$_x$ works equally well with either NO or NO$_2$ in the feed gas. However, this fact does not tell us anything about the importance of step 1 in the proposed reaction scheme, because at the temperatures used here, there is a quasi-equilibrium between NO and NO$_2$ in the gas bulk. This can be seen in Figs. 1a and 1b which show very similar NO and NO$_2$ levels at temperatures above 250°C with either NO or NO$_2$ in the feed. This is the result of the fairly low flow relative to the number of sites active for NO oxidation and reduction. When comparing Figs. 1, 3, and 7 it can be seen that the temperature dependence of the NO-to-NO$_2$ oxidation does not directly follow the NO$_x$ storage rate. It is, however, likely that the temperature dependence of the NO oxidation is important for NO$_x$ storage at temperatures below 450°C. The decrease in NO$_x$ storage at higher temperatures probably has to do with the stability of the metal nitrate in which the NO$_x$ is stored. A further indication of the importance of NO$_2$ is the high adsorption yield at room temperature seen in Fig. 6c. The reason that no storage is observed above 500°C is most probably that NO$_x$ desorbs around 480°C (see Fig. 6b).

The slow increase in NO$_x$ stored with increasing oxygen content seen in Figs. 4 and 8 is consistent with a storage step involving oxygen. The variation in the amount of NO$_x$ stored with propene content (Table 4) is probably connected both to the different temperatures in the catalysts, caused by the different reaction heat dissipated at different C$_3$H$_6$ flows, and to the somewhat lower oxygen coverages at high propene concentration.

Considering that effective NO$_x$ storage requires the presence of noble metals, it can be assumed that the presence of atomic oxygen is important for the process. This species is present in steps 3, 4a, and 4b. However, the storage–release cycles cannot be seen for a sample without noble metals (i.e., a BaO/Al$_2$O$_3$ sample) even if NO$_x$ is in the form of NO$_2$. This indicates that the reaction step in which the NO$_x$ is stored really includes atomic oxygen and thus probably is in the form of step 4a or 4b. Alternatively, atomic oxygen activates the barium surface into a form that readily takes up NO$_x$.

As mentioned under Results, we observe effective storage (i.e., the process where NO$_x$ is stored during the lean phase and the catalyst is regenerated during the rich phase) only for the catalyst with noble metals, barium oxide, and alumina, and not for the samples without either noble metals or barium oxide. The Pt–Rh/Al$_2$O$_3$ sample shows no storage except for small amounts at low temperatures (300°C), where NO$_x$ adsorbs onto the alumina, which also can be seen in Fig. 1b where a NO$_x$ desorption peak is recorded at 175C°. At these temperatures, there is also a fair amount of continuous reduction of NO$_x$ to N$_2$ and N$_2$O by propene (16). The TPD experiments for this catalyst show that NO is readily reduced on a prereduced sample while the preoxidized sample give desorbing NO and O$_2$ around 400°C, probably originating from NO$_2$ desorbing from noble metal sites. The FTIR measurements for this sample (9) show several peaks from nitrates adsorbed on alumina (16) but lack several features present for the full NO$_x$ storage catalyst. The NO$_2$ TPD spectrum shows that large amounts of NO$_2$ stick to the Al$_2$O$_3$ and desorb in two peaks at 120 and 350°C. It should be noted that this NO$_2$ is adsorbed on an oxidized catalyst since the sample is oxidized by NO$_2$ even at room temperatures. During lean–rich cycles at 400°C, as in Fig. 2b, the rate of desorption of NO$_2$ from Al$_2$O$_3$ is very rapid as seen in Fig. 6f. This means that no effective storage takes place during the lean period for a Pt–Rh/Al$_2$O$_3$ sample. At lower temperatures, for example, around 250°C, one would expect from Fig. 6f that NO$_2$ adsorbs on Al$_2$O$_3$ during the lean phase. This is also what we observed experimentally.

Even when using NO$_x$ in the form of NO$_2$, no effective storage can be observed for the BaO/Al$_2$O$_3$ sample at 400°C. As mentioned above, the reason for this may be that no atomic oxygen is present which prevents storage according to reaction steps 4a and 4b. The reason can also be that this sample is not regenerated from adsorbed NO$_2$ during the rich phase. Thermal desorption does not take place until $T > 450$°C (see Fig. 6i) and because of the absence of noble metals, the nitrogen oxides will not be reduced by the propene. It is interesting that about three times more NO adsorbs on the preoxidized sample compared with the

prereduced sample, although we do not see NO_2 desorbing (Fig. 6h). This indicates that oxygen present in the preoxidized sample takes part in the surface bonding of NO.

Under reducing conditions two important things take place. The oxygen is turned off and therefore the rate of storage of NO_x (step 4) becomes small while the rate of the reverse reaction (step 5) initially remains high so that relatively more NO_x is present on the surface. Second, the noble metal sites are reduced which leads to the dissociation and reduction of NO_x in step 7 (which is just an example of many possible pathways of NO_x reduction). The importance of the sites being reduced for step 7 to take place is well known (17) and clearly demonstrated in the TPD measurements (Fig. 6) where recombination of dissociated NO to N_2 and N_2O takes place only on the prereduced sample in NO TPD.

The magnitude of the isocyanate peak during the regeneration phase (Fig. 7) maximizes in the temperature interval 370–450°C, i.e., the same interval where the NO_x storage reaches a maximum. This can be interpreted as large amounts of NO_x becoming available for the formation of isocyanate with propene during the rich period (18).

From Fig. 5 and Table 7 it is clear that the presence of NO during the rich phase prevents, to a large extent, the regeneration of the NO_x storage catalyst. Regeneration with only propene results in about twice as much stored NO_x in the following lean phase, and even thermal regeneration in pure N_2 works better than regeneration in NO/C_3H_6. Somehow the decomposition of barium nitrate seems to be hindered by NO. One possibility is that Pt sites needed for this decomposition are occupied by NO despite the high surplus of propene during the rich period. One other possibility is that barium remains in an activated state where it can react with NO in the absence of oxygen. In that case the effective decomposition will be slower with NO present due to continuous formation of nitrates.

With respect to the nature of the stored NO_x it is known that several complex compounds, e.g., barium aluminates and nonstoichiometric compounds, may have NO_x storage capacity under lean reaction conditions (19). Several surface complexes containing barium, alumina, and nitrogen oxides, rather than bulk species, may also be formed. The nature of such complexes is difficult to elucidate. NO_x may therefore be strongly bound on the catalyst surface and in the surface layers of the catalyst in several types of species. It is likely that NO_x storage proceeds via surface-bound nitrite and nitrate compounds to barium nitrate. On the basis of experiments performed in this study, the formation of $Ba(NO_3)_2$ under lean conditions seems to be a plausible reaction step of major importance under lean NO_x storage and reduction reactions.

Two different types of breakthrough peaks are observed in the experiments. There is an HC peak when switching from rich to lean conditions. To understand this peak we must remember that the oxygen is turned off during the rich phase; i.e., there is only a low rate of combustion, NO_x being the only oxidizing agent, which is manifested in the decrease in the catalyst temperature. When the oxygen is turned on, there will be a moving combustion front in the catalyst as the adsorbed hydrocarbons are oxidized. This will result in local hot zones where adsorbed HC will thermally desorb up to the point where the (local) oxygen coverage becomes high enough for all HC to react with oxygen.

The NO_x breakthrough peaks when switching from lean to rich conditions is discussed by Bögner et al. (7) in terms of a relatively slow reduction of noble metal sites compared with the decomposition of the barium nitrate, giving a sudden increase in the surface coverage of NO_x. However, against this view can be argued that we also observe these peaks without a storage component in the catalyst. We rather believe that these peaks are caused by a rapid reduction of noble metal sites. In this process, the adsorption properties of NO_x on the noble metal surface change radically. Root et al. have shown that coadsorption of oxygen and NO on Rh(111) lowers the desorption temperature for NO compared with NO adsorbed on a clean Rh(111) surface (20). This is manifested in the TPD results in Fig. 6. For the oxidized samples, the desorption of NO and O_2 takes place above 400°C. For the reduced sample, on the other hand, NO desorbs as N_2 and N_2O at much lower temperatures. The switch from a lean to a rich atmosphere causes a transformation to a surface where no NO_x is adsorbed at these temperatures (400°C). This is also manifested in Fig. 4 where the peaks can be seen to decrease with decreasing O_2 content. This can be understood as follows: At lower O_2 content relatively more propene reacts with NO_x rather than with O, leading to lower NO_x coverage. Further, different storage times do not affect the magnitude of the peaks. Another important factor leading to these breakthrough peaks is that when oxygen is turned off, the rate of step 4 becomes small while the rate of step 5 is initially high. This should give increased coverage of NO_x on the noble metal sites leading to, for a short period, a higher rate of desorption of NO_x.

We thus believe that the reduction of noble metal sites is fast and therefore that the rate-limiting step during the rich phase is the decomposition of the barium nitrate.

5. CONCLUSIONS

We have presented a systematic investigation of the effect on NO_x storage in a model $Pt–Rh/BaO/Al_2O_3$ catalyst of several parameters. The investigations are compared with corresponding results for samples without noble metals or barium oxide, respectively. Significant amounts of NO_x were found to be stored in the catalysts containing both barium oxide and noble metals. For these catalysts the following observations were made: (1) a maximum in NO_x

storage was observed at about 380°C; (2) around this temperature no significant differences between NO and NO$_2$ with respect to NO$_x$ storage capacity could be observed; (3) a slow increase in the amount of NO$_x$ stored could be observed with increasing oxygen concentration during the lean phase; (4) significant NO$_x$ desorption peaks, mainly of NO, were observed immediately after the switch from lean to rich conditions; and (5) at about 380°C the *in situ* FTIR spectra showed characteristic nitrate peaks in the region 1300–1400 cm^{-1} when NO$_x$ catalysts were stored under lean conditions and isocyanate peaks around 2230 cm^{-1} when the catalysts were regenerated under rich conditions, in the presence of hydrocarbons. The reaction step leading to stored NO$_x$ is believed to involve NO$_2$ and the presence of atomic oxygen. During the rich period, the noble metal surfaces are probably reduced, leading to breakthrough peaks when NO desorbs.

REFERENCES

1. Heck, R. M., and Farrauto, R. J., "Catalytic Air Pollution Control." Van Nostrand Reinhold, New York, 1995.
2. Shelef, M., *Chem. Rev.* **95**, 209 (1995).
3. Burch, R., and Millington, P. J., *Catal. Today* **26**, 185 (1995).
4. Iwamoto, M., and Hamada, H., *Catal. Today* **10**, 51 (1991).
5. Miyoshi, N., Matsumoto, S., Katoh, K., Tanaka, T., Harada, J., Takahashi, N., Yokota, K., Sugiura, M., and Kasahara, K., SAE Technical Paper Series, No. 950809 (1995).
6. Takahashi, N., Shinjoh, H., Iijima, T., Suzuki, T., Yamazaki, K., Yokota, K., Suzuki, H., Miyoshi, N., Matsumoto, S., Tanizawa, T., Tanaka, T., Tateishi S., and Kasahara, K., *Catal. Today* **27**, 63 (1996).
7. Bögner, W., Krämer, M., Krutzsch, B., Pischinger, S., Voigtländer, D., Wenninger, G., Wirbeleit, F., Brogan, M. S., Brisley, R. J., and Webster, D. E., *Appl. Catal. B* **7**, 153 (1995).
8. Machida, M., Yasuoka, K., Eguchi, K., and Arai, H., *J. Chem. Soc. Chem. Commun.* **17**, 1165 (1990).
9. Fridell, E., Skoglundh, M., Johansson, S., Westerberg, B., Törncrona, A., and Smedler, G., *Stud. Surf. Sci. Catal.* **116**, 537 (1998).
10. Skoglundh, M., Johansson, H., Löwendahl, L., Jansson, K., Dahl, L., and Hirschauer, B., *Appl. Catal. B* **7**, 299 (1996).
11. Lööf, P., Kasemo, B., and Keck, K.-E., *J. Catal.* **118**, 339 (1989).
12. Lundgren, S., Keck, K.-E., and Kasemo, B., *Rev. Sci. Instrum.* **65**, 2696 (1994).
13. Persson, H., *et al.*, to be published.
14. Summers, and Baron, *J. Catal.* **57**, 380 (1979).
15. Davydov, A. A., "Infrared Spectroscopy of Adsorbed Species on the Surface of Transition Metal Oxides." Wiley, Chichester, 1990.
16. Acke, F., Westerberg, B., Eriksson, L., Johansson, S., Skoglundh, M., Fridell, E., and Smedler, G., *Stud. Surf. Sci. Catal.* **116**, 285 (1998).
17. Ansell, G. P., Golunski, S. E., Hayes, J. W., Walker, A. P., Burch, R., and Millington, P. J., *Stud. Surf. Sci. Catal.* **96**, 255 (1995).
18. Acke, F., Westerberg, B., and Skoglundh, M., *J. Catal.* **179**, 528 (1998).
19. Machida, M., Yasuoka, K., Eguchi, K., and Arai, H., *J. Chem. Soc. Chem. Commun.* **17**, 1165 (1990).
20. Root, T. W., Schmidt, L. D., and Fisher, G. B., *Surf. Sci.* **134**, 30 (1983).